Interactions between Steady Non-Uniform Currents and Gravity Waves with Applications for Current Measurements[1]

NORDEN E. HUANG,[2] DAVIDSON T. CHEN[2] AND CHI-CHAO TUNG[3]

North Carolina State University, Raleigh 27607

AND JAMES R. SMITH

Research Triangle Institute, Research Triangle Park, North Carolina

(Manuscript received 28 January 1972, in revised form 29 May 1972)

ABSTRACT

Interactions between steady non-uniform currents and gravity waves are generalized to include the case of a random gravity wave field. The Kitaigorodskii-Pierson-Moskowitz frequency spectrum is used as the basic spectral form for zero current condition. Modified spectral functions in both wavenumber and frequency spaces under the influence of current are found by using energy conservation and kinematic wave conservation laws. The relative importance of the current-wave interaction was measured by the nondimensional parameter U/C_0, with U as the current speed and C_0 the phase speed of a wave under no current. As a result of the current-wave interaction, the magnitude and the location of the energy peak in the spectrum is altered.

Since the phase speed of gravity waves is a monotonically decreasing function of wavenumber and frequency, the influence of current will be predominant at the higher wavenumber range. Furthermore, the contribution from the higher wavenumber range dominates the surface slope spectrum; the current conditions changes the surface slope pattern drastically. This phenomenon is studied by use of Phillips' equilibrium range spectrum in wavenumber space. It was found that the rms surface slope is extremely sensitive to the change of current conditions especially for the case of adverse current, but eventually becomes saturated at a high positive value. The surface slope data together with a generalized dispersion relation offer a possible current measurement technique which appears ideally suited for remote sensing devices such as stereoscopic photography and radar scattering.

1. Introduction

Since there is no other motion more common than surface waves, on the surface of the ocean, the study of waves has been of central concern for oceanographers. Since surface waves belong to a particular group of motion in which the fluid particles are organized in such a way as to show the oscillatory surface elevation, any concurrent motion in the fluid will produce interactions; for example, wave-wave interactions (Phillips, 1960, 1966) and wave-current interactions (Taylor, 1955; Ursell, 1960; Whitham, 1960, 1962; Longuet-Higgins and Stewart, 1960, 1961). From these interactions, certain changes in the wave characteristics will arise such as changes in wave amplitude (Longuet-Higgins and Stewart, 1960, 1961) and in phase speed (Longuet-Higgins and Phillips, 1962; Phillips, 1966). Most of the previous studies, however, are centered around the nonlinear dynamic effects which are primarily changes due to the weak "amplitude dispersion." The kinematic influences, on the other hand, could produce first-order changes in the wave characteristics by "frequency dispersion." Though most of the important ideas on wave kinematics have been explained by Lighthill and Whitham (1955), Landau and Lifshitz (1959), Ursell (1960), Whitham (1960) and Longuet-Higgins and Stewart (1961), few practical applications have ever been attempted. In this paper, we will concentrate on the particular kinematic aspects of the influence of currents on waves: the dispersion relationship, the dynamic consequences on the modification of the spectral function, and a possible application to current measurement.

In order to present the analysis, a brief account of the previous results and some definitions will be given first.

Let a component of a general wave field be specified by

$$\zeta(\mathbf{x},t)=a(\mathbf{x},t)e^{i\chi(\mathbf{x},t)}, \tag{1}$$

where $a(\mathbf{x},t)$ is the amplitude and $\chi(\mathbf{x},t)$ the phase function; both are functions of space $\mathbf{x}$ and time t in general. With this expression, the wavenumber $\mathbf{k}$ and frequency

[1] Presented at the Conference on the Interaction of the Sea and the Atmosphere, 1–3 December 1971, Ft. Lauderdale, Fla.

[2] Dept. of Geosciences.

[3] Dept. of Civil Engineering.

n can be defined by

$$\left.\begin{aligned}\mathbf{k}&=\nabla\chi\\ n&=-\frac{\partial\chi}{\partial t}\end{aligned}\right\}. \tag{2}$$

Combining the two expressions in Eq. (2), we have the kinematic conservation law of waves as

$$\frac{\partial\mathbf{k}}{\partial t}+\nabla n=0. \tag{3}$$

Here the wavenumber is the same as in the usual definition of $2\pi/\lambda$ with λ as the wavelength. The frequency n, however, is not the same as in a pure oscillatory wave; rather, it represents the total frequency which is the frequency actually observed. For wave motion coupled with a current, the total frequency can be decomposed into two parts, namely, the intrinsic frequency σ and the convective frequency, i.e.,

$$n=\mathbf{k}\cdot\mathbf{U}(\mathbf{x},t)+\sigma, \tag{4}$$

where $\mathbf{U}(\mathbf{x},t)$ is the current velocity vector.

For a steady state, Eq. (3) reduces to

$$\nabla n=0. \tag{5}$$

This implies that the total frequency of the wave motion is an invariant under steady state. Then Eqs. (4) and (5) give us

$$n=\mathbf{k}\cdot\mathbf{U}(\mathbf{x},t)+\sigma=\sigma_0, \tag{6}$$

where the subscript indicates the state when there is no current.

If the weak nonlinear dynamic interaction is neglected for the time being, we have

$$\left.\begin{aligned}\sigma^2&=gk\\ c^2&=\frac{g}{k}\end{aligned}\right\}, \tag{7}$$

where c is the phase speed and g the gravitational acceleration.

Without loss of generality, we can assume a one-dimensional case. The energy conservation becomes

$$E\left(\frac{c}{2}+U\right)c=\tfrac{1}{2}E_0c_0^2=\text{constant}, \tag{8}$$

where E is the wave energy. With these equations, it has been shown that (see, e.g., Phillips, 1966, p. 57ff)

$$\frac{c}{c_0}=\tfrac{1}{2}+\tfrac{1}{2}\left(1+\frac{4U}{c_0}\right)^{\frac{1}{2}}=\left(\frac{k_0}{k}\right)^{\frac{1}{2}}, \tag{9}$$

$$\frac{a}{a_0}=\left(\frac{c}{c+2U}\right)^{\frac{1}{2}}, \tag{10}$$

where a is wave amplitude.

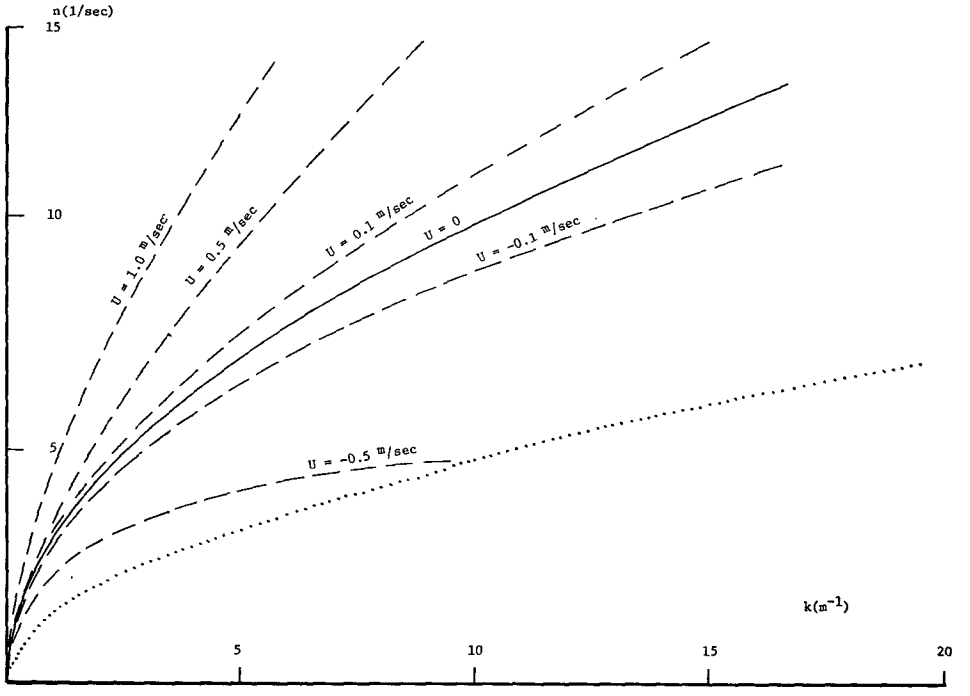

FIG. 1. Influence of current on the dispersion relationship. The dotted line corresponds to the limiting condition for which the group speed equals $-U$.

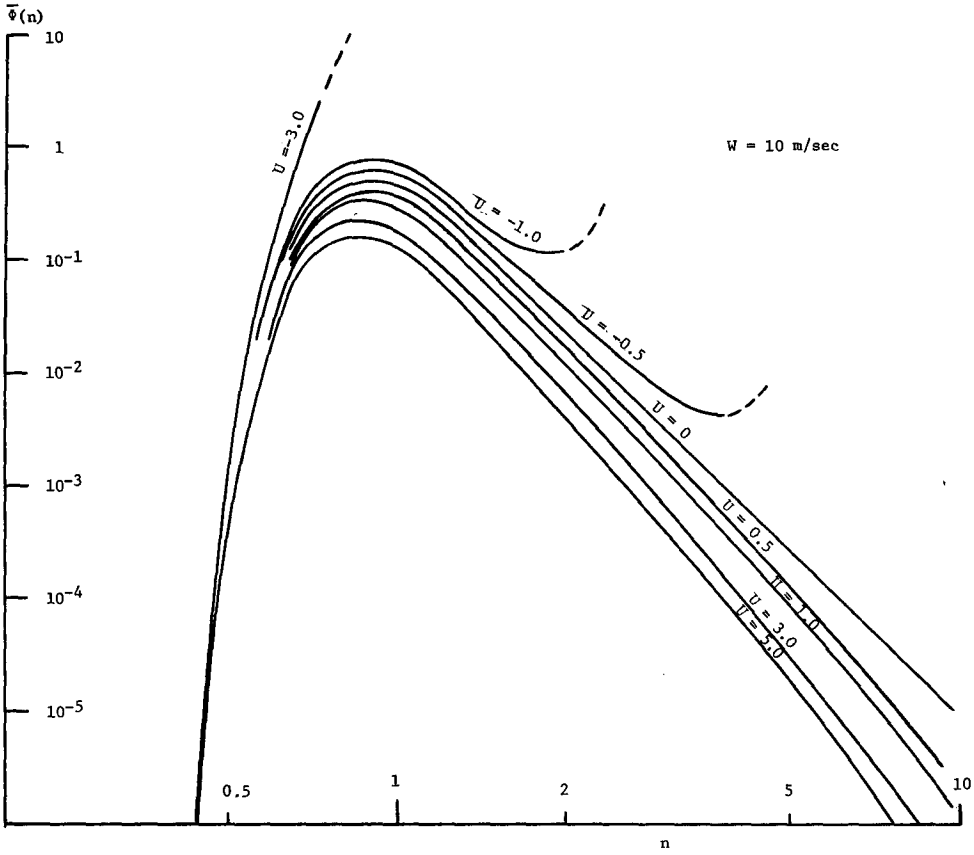

FIG. 2. Changes of frequency spectra for 10 m sec^{-1} wind, under different current conditions: $\bar{\phi}(n)$ in m^2 sec, n in rad sec^{-1} and U in m sec^{-1}.

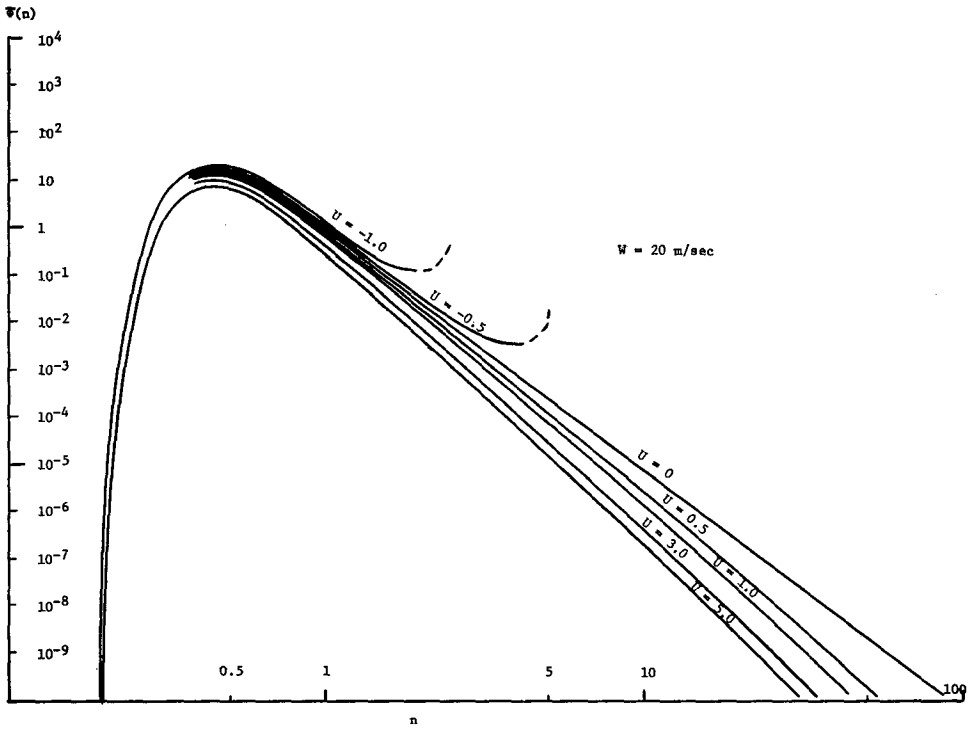

FIG. 3. As in Fig. 2 except for a 20 m sec^{-1} wind.

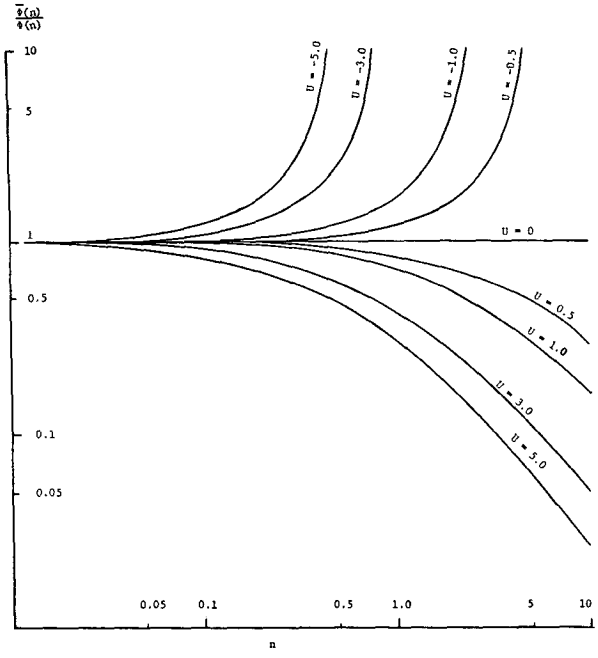

FIG. 4. Relative changes of frequency spectra under different current conditions: U in m sec^{-1} and n in rad sec^{-1}.

Combining Eqs. (6), (7) and (9), we have

$$gk=\frac{n^2}{\left[\frac{1}{2}+\frac{1}{2}\left(1+\frac{4Un}{g}\right)^{\frac{1}{2}}\right]^2}. \tag{11}$$

This provides us with a more general form of the dispersion relationship including the influence of currents. The result is shown in Fig. 1, using U as a parameter. The dotted line indicates the theoretical limit when the group velocity is equal to the negative current velocity. No wave can exist beyond this line. In fact, waves will break long before they approach this limit, because the amplitude would be infinite at this critical velocity. By comparing this result with the effects of nonlinear wave-wave interaction as reported by Huang and Tung (1972), it is obvious that the frequency dispersion offered a much stronger modification.

2. Energy spectra

Having briefly recounted the effect of current on a single wave, we want to see the effect of current on a random wave field, i.e., on spectral functions. To begin with, let us assume that the ocean wave field is represented by the Kitaigorodskii (1962)-Pierson-Moskowitz (1964) spectrum

$$\phi(n)=\frac{\beta g^2}{n^5}\exp[-\alpha(n_0/n)^4], \tag{12}$$

where n is the frequency, α,β are non-dimensional constants equal to 0.74 and 0.81×10^{-2}, respectively, and $n_0=g/W$ with W as the mean wind speed. In a particular frequency band, energy can be expressed as $\phi(n)dn$. When the waves propagate into a region with current, the energy contained in that particular frequency band will change through interchange of energy between waves and current. If we let the energy density of the waves under current be $\bar{\phi}(n)dn$, then by Eq. (8), we have

$$\tfrac{1}{2}c_0^2\phi(n)dn=\left(\frac{c}{2}+U\right)c\bar{\phi}(n)dn. \tag{13}$$

Now, by Eq. (5), we concluded that n is an invariant. Therefore,

$$\bar{\phi}(n)=\frac{\frac{1}{2}c_0^2}{\left(\frac{c}{2}+U\right)c}\phi(n). \tag{14}$$

By using Eq. (9), and some simplification, we finally have

$$\bar{\phi}(n)=\frac{4\frac{\beta g^2}{n^5}\exp[-\alpha(n_0/n)^4]}{\left[1+\left(1+\frac{4Un}{g}\right)^{\frac{1}{2}}\right]\left[\left(1+\frac{4Un}{g}\right)^{\frac{1}{2}}+\left(1+\frac{4Un}{g}\right)\right]}. \tag{15}$$

This gives an expression for the frequency spectrum under the influence of current.

For $W=10$ and 20 m sec^{-1}, Eq. (15) is plotted in Figs. 2 and 3 with U as a parameter. In each figure, whenever the current speed is negative, the energy density shows a cutoff frequency. This cutoff frequency can be calculated easily from Eq. (15) by requiring that

$$1+\frac{4Un}{g}\geqslant 0, \tag{16}$$

so that the energy density will be a real quantity. In case Eq. (16) equals zero, $\bar{\phi}(n)$ will approach infinity. This condition corresponds physically to the wave-breaking phenomenon discussed in the Introduction for a single wave. In actual cases, the spectrum will show an overshoot or energy pile-up at the frequency just below that given by Eq. (16), and the sea state becomes extremely rough caused by the breaking. In addition, the energy density at a frequency higher than this cutoff point is much lower than would be the case without current. A non-dimensional ratio

$$\frac{\bar{\phi}(n)}{\phi(n)}=\frac{4}{\left[1+\left(1+\frac{4Un}{g}\right)^{\frac{1}{2}}\right]\left[\left(1+\frac{4Un}{g}\right)^{\frac{1}{2}}+\left(1+\frac{4Un}{g}\right)\right]}, \tag{17}$$

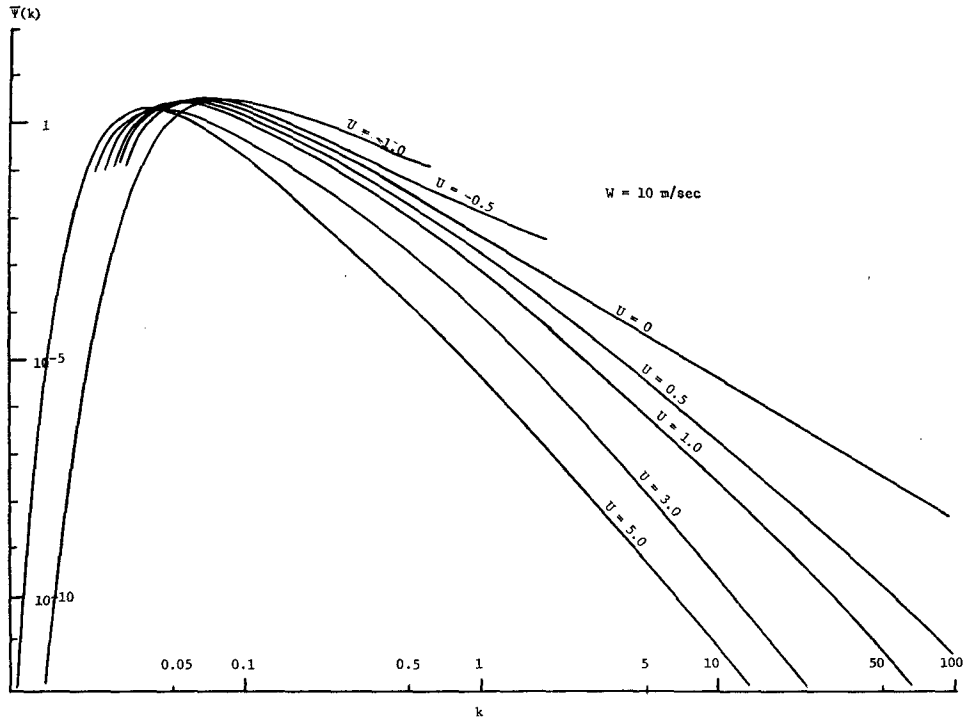

FIG. 5. Changes of wavenumber spectra for a 10 m sec^{-1} wind, under different current conditions: $\bar{\psi}(k)$ in m^3, k in m^{-1} and U in m sec^{-1}.

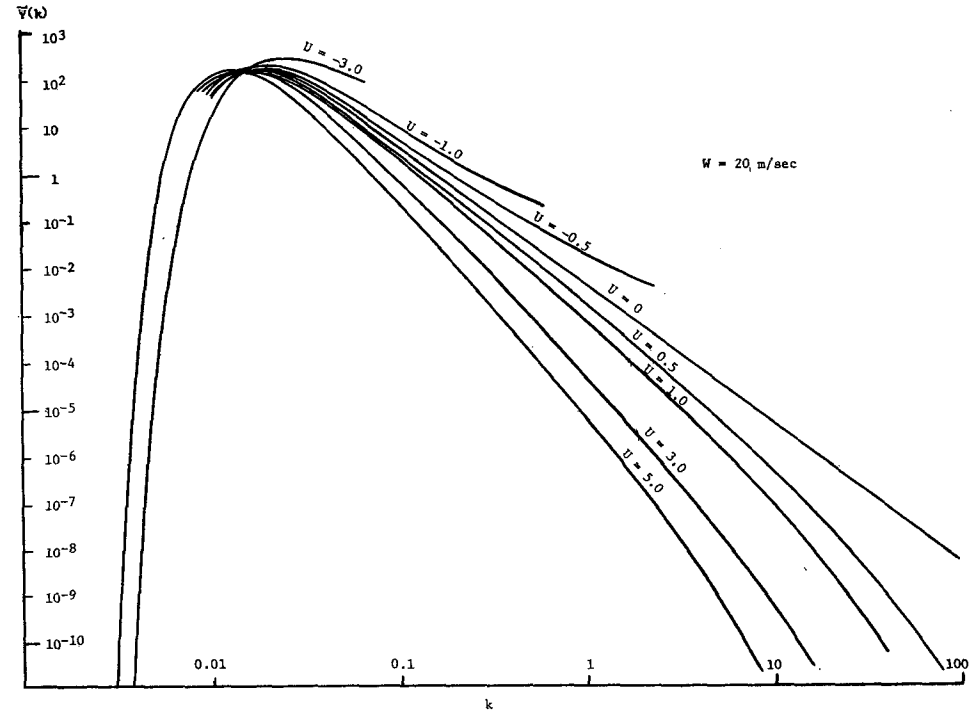

FIG. 6. As in Fig. 5 except for a 20 m sec^{-1} wind.

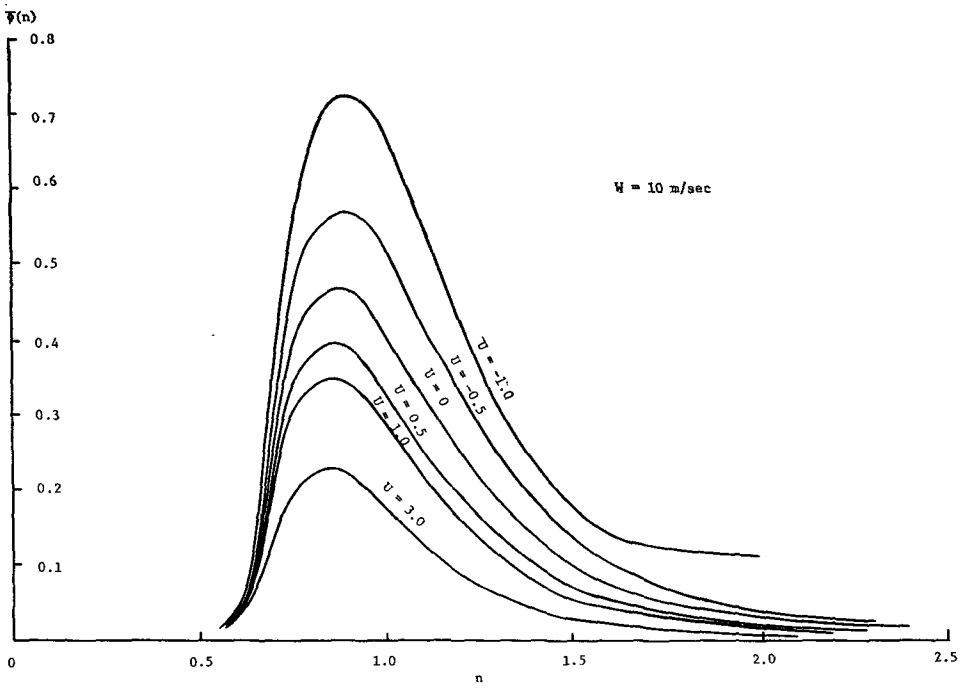

FIG. 7. Changes of frequency spectra for a 10 m sec^{-1} wind under different conditions (linear scale for $\bar{\phi}$).

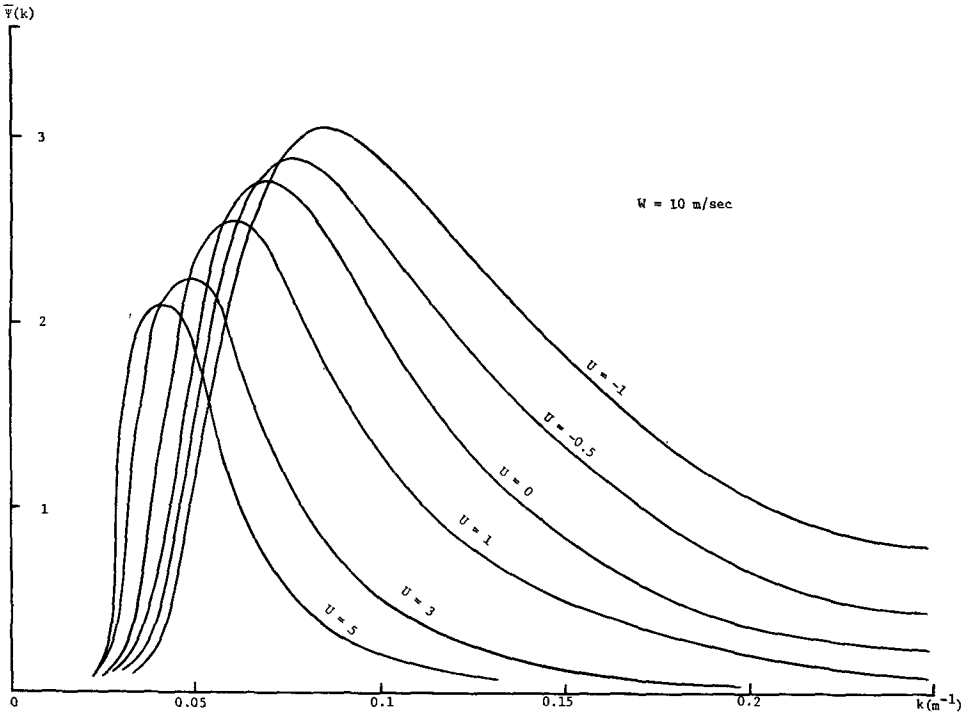

FIG. 8. Changes of wavenumber spectra for a 10 m sec^{-1} wind under different current conditions (linear scale for $\bar{\psi}$).

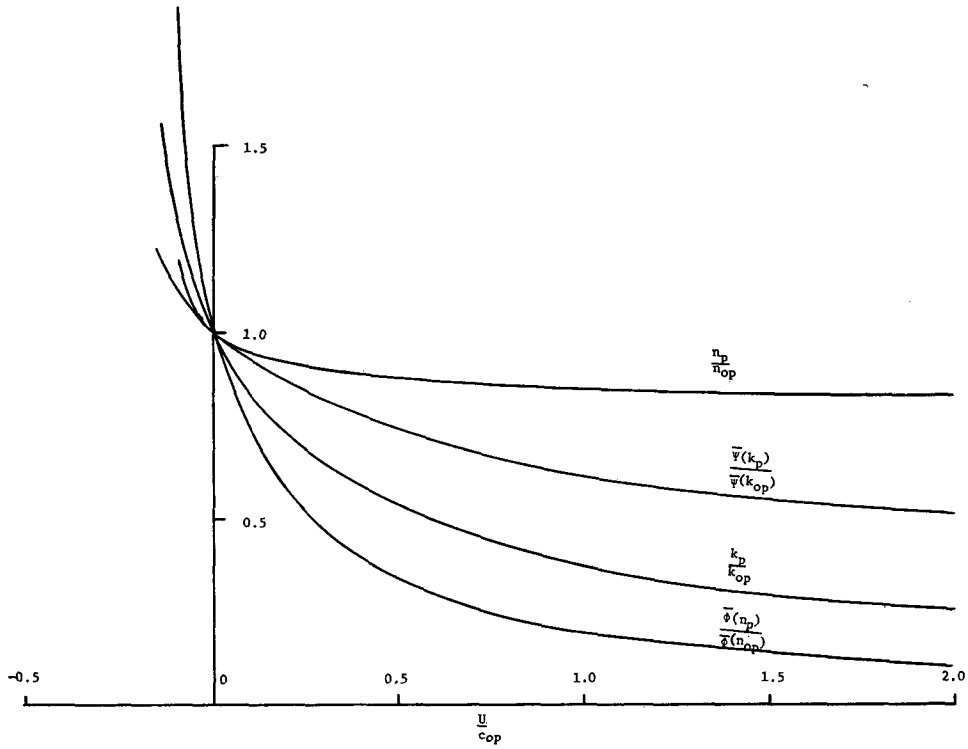

FIG. 9. Ratios of the change in peak location and peak magnitude for both frequency and wavenumber spectra under different current conditions.

is shown in Fig. 4 in which the change in energy density at different frequency bands under various current conditions is clearly shown.

Having obtained the modified frequency spectrum, we can use the generalized dispersion relationship to convert frequency spectra into wavenumber spectra. By energy considerations, we have

$$\bar{\phi}(n)dn=\bar{\psi}(k)dk, \tag{18}$$

where $\bar{\phi}(k)$ is the wavenumber spectrum and

$$dn=\left(U+\frac{c}{2}\right)dk$$

as derived from Eqs. (6) and (7). Hence,

$$\bar{\psi}(k)=\frac{\beta}{2\left(1+\frac{U}{c}\right)^7}\frac{1}{k^3}\exp\left[-\alpha\left(\frac{n_0}{k(U+c)}\right)^4\right]. \tag{19}$$

Typical cases for $\bar{\psi}(k)$ are plotted in Figs. 5 and 6. Since the dispersion relationship is invalid for $U<-c/2$, the spectral function in wavenumbers will also have a cutoff point as shown.

In order to show the dynamic consequence of the current-wave interaction in more detailed form, spectra for the wind speed $W=10$ m sec^{-1} case are plotted on a linear scale in Figs. 7 and 8. These figures clearly show the changes in the peak location and magnitude in the frequency and wavenumber spectra. Fig. 9 summarizes the essential features in Figs. 7 and 8 by plotting the changes of peak location and magnitude of the frequency and wavenumber spectra as functions of U/c_{op}, where c_{op} is the speed of the waves corresponding to peaks of the frequency or wavenumber spectrum under no current.

In addition to the frequency and wavenumber spectra, the surface slope spectra can also be obtained as

$$S(k)=k^2\bar{\psi}(k). \tag{20}$$

The result is shown in Figs. 10 and 11. A definite trend of increasing surface roughness is clearly seen when waves are propagating from a region of no current into an opposing current. The change could be used to explain the drastically different sea states that result under an opposing wind along major current systems with a sharp boundary such as the Gulf Stream, and it could also be used to deduce current information from wave measurements as will be discussed in a later section.

3. Energy spectra in the equilibrium range

The effect of current on wave spectra is clearly shown in the previous section. In all the calculations, the ratio of U/c is an important scale to measure the effects of the current. Since the phase speed for a gravity wave is a

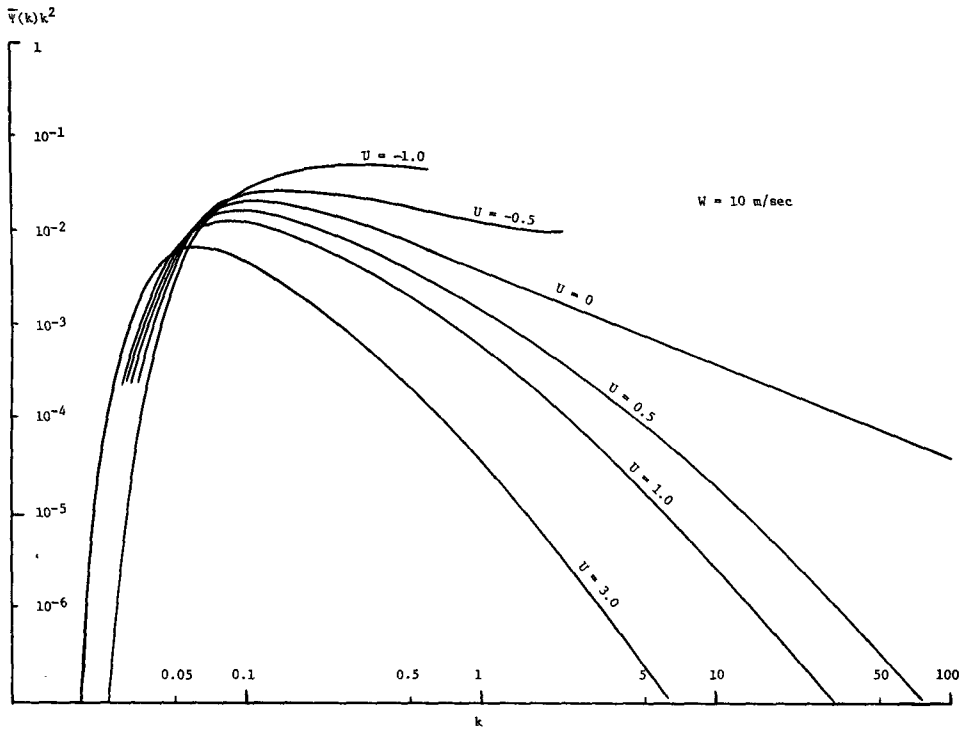

FIG. 10. Changes of surface slope spectra for a 10 m sec^{-1} wind under different current conditions.

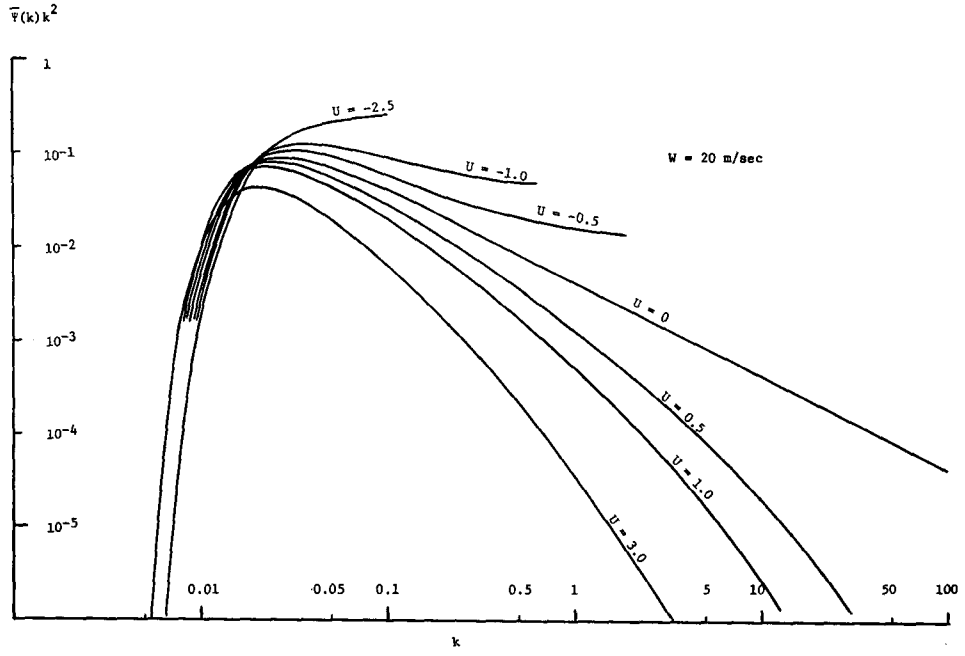

FIG. 11. Changes of surface slope spectra for a 20 m sec^{-1} wind under different current conditions.

monotonically decreasing function of wavenumber, the ratio U/c will increase, or the relative importance of the current will become more pronounced, in the high as compared to the low wavenumber or frequency range of the spectrum. As a consequence, the wave energy spectra in the equilibrium range will have to be modified. This modification can be shown either by starting with Phillips (1958) equilibrium spectrum

$$\left.\begin{aligned}\phi(n)&=\beta g^2 n^{-5}, \quad n_r\gg n\gg n_p\\ \psi(k)&=Bk^{-3}, \quad k_r\gg k\gg k_p\end{aligned}\right\}, \tag{21}$$

and following the argument used in the previous section, or by passing to the limit of high wavenumber or frequency in Eqs. (14) and (19). Here n_r and k_r are the typical frequency and wavenumber of capillary waves, and n_p and k_p the frequency and wavenumber at the spectrum peak. Either way, we obtain

$$\bar{\phi}(n)=\beta' g^2 n^{-5},$$

where

$$\beta'=\frac{4\beta}{\left[1+\left(1+\frac{4U}{c_0}\right)^{\frac{1}{2}}\right]\left[\left(1+\frac{4U}{c_0}\right)+\left(1+\frac{4U}{c_0}\right)^{\frac{1}{2}}\right]}. \tag{22}$$

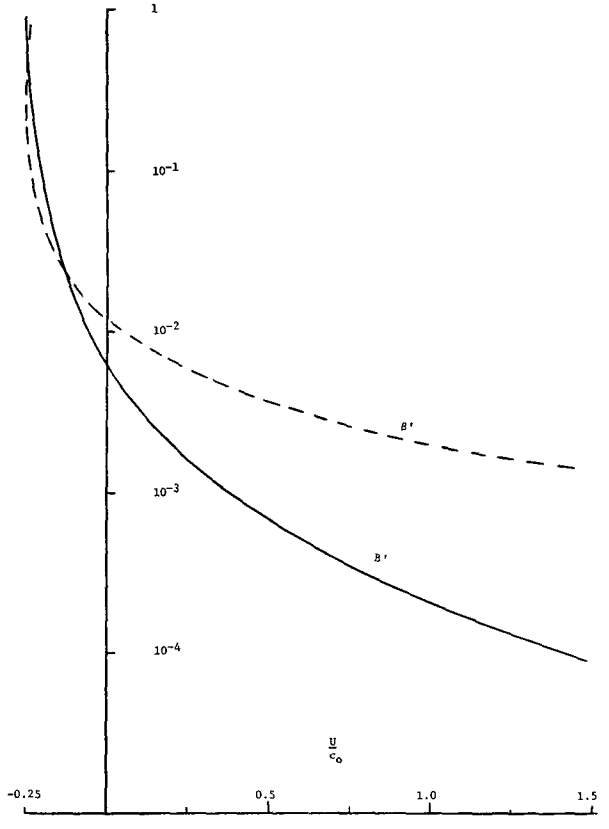

FIG. 12. Variation of equilibrium range spectra constants with current conditions.

The value of β' is plotted against U/c_0 in Fig. 12. When $U=0$, we get $\beta'=\beta$ as expected.

For a wavenumber spectrum, we have

$$\bar{\psi}(k)=B'k^{-3},$$

where

$$B'=\frac{\beta}{2\left[1+\frac{2U/c_0}{1+\left(1+\frac{4U}{c_0}\right)^{\frac{1}{2}}}\right]^7}. \tag{23}$$

The value of B' is also shown in Fig. 12. Again, when $U=0$, we have

$$B'=\frac{\beta}{2}=B, \tag{24}$$

which is exactly the conversion given by Phillips (1966).

Since both B' and β' are functions of U/c_0, the change of either U or c_0 will change the value of B' and β'. Furthermore, since c_0 is a function of wavenumber or frequency, B' and β' will also become wavenumber or frequency dependent. The general relationship between B' and β' is given by B'/β' shown in Fig. 13. From these figures, it becomes obvious that the value of B' varies over a much wider range than β' over the same U/c_0 range. This is probably one of the reasons for the scattering in all the field measurements on B'.

4. Application for current measurement

In the open ocean, the cutoff wavenumber for the equilibrium range at the lower end is very close to the spectral peak, $k_0=g/W^2$, with W as the wind speed; at the high wavenumber end it is controlled by viscosity or capillarity. Since the major contribution to the surface slope comes from higher wavenumbers, the equilibrium range spectrum will give a very good approximation. Using such an approximation, Phillips (1966) showed that

$$\overline{(\nabla\zeta)^2}=\int_k k^2\psi(k)dk=B\log\frac{k_c}{k_0}, \tag{25}$$

where k_c is the cutoff frequency at the higher end. If we concentrate on the gravity wave case only, then k_c will be determined by the capillary force. As in the field study by Cox and Munk (1954a, b), where waves <30 cm were entirely damped out by an artificially induced slick, we then have

$$\overline{(\nabla\zeta)^2}=B\log(k_cW^2/g). \tag{26}$$

Therefore, the surface roughness, $\overline{(\nabla\zeta)^2}$, is purely a function of wind speed. This result is based on wave motion alone. If the wave motion encounters a concurring current, the characteristics of the waves will be different as a consequence of the kinematic and dynamic

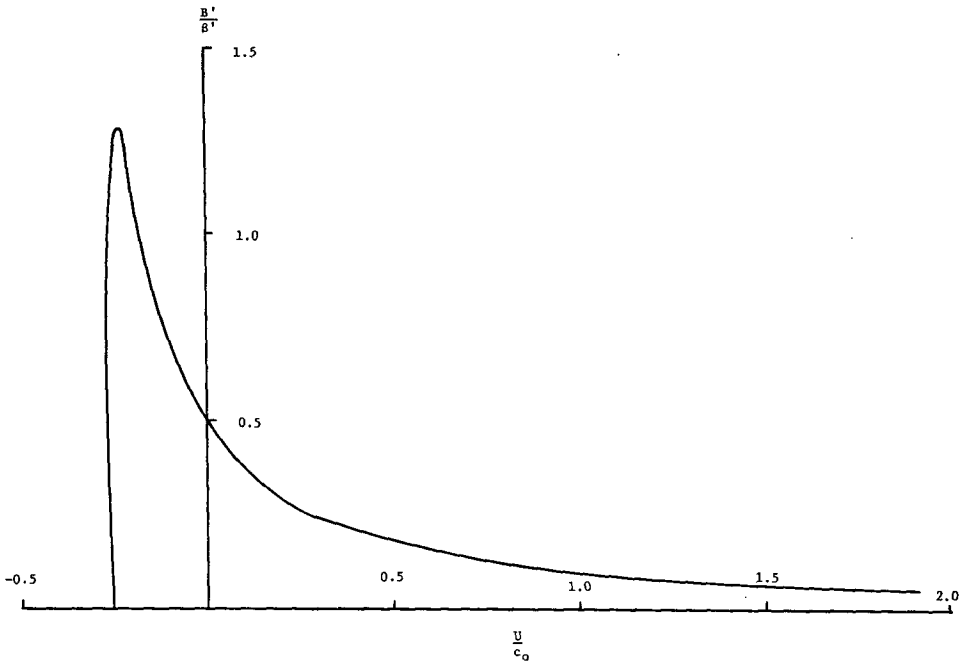

FIG. 13. Ratio of equilibrium range spectra constants current conditions.

interaction shown in the previous sections. The surface roughness, in this case, is

$$\overline{(\nabla\zeta)^2}=\int_{k_0}^{k_c}\frac{\beta}{2\left(1+\frac{U}{c}\right)^7}\frac{dk}{k}$$

$$=-\beta\left[\log|U+c|+\frac{6U}{U+c}-\frac{15U^2}{2(U+c)^2}+\frac{20U^3}{3(U+c)^3}-\frac{15U^4}{4(U+c)^4}+\frac{6U^5}{5(U+c)}-\frac{U^6}{6(U+c)^6}\right]$$

$$=\beta\left\{\log\left|\frac{U+c_0}{U+C_c}\right|+6\left(\frac{U}{U+C_0}-\frac{U}{U+C_c}\right)-\frac{15}{2}\left[\left(\frac{U}{U+C_0}\right)^2-\left(\frac{U}{U+C_c}\right)^2\right]+\cdots\right\}, \quad (27)$$

where C_c is the phase speed corresponding to the wave with cutoff wavenumber k_c. When $U=0$, every term in the parentheses in Eq. (27) is zero except the first which reduces to

$$\overline{(\nabla\zeta)^2}=\beta\log\left|\frac{c_0}{c}\right|=\frac{\beta}{2}\log\left(\frac{k_c}{k_0}\right). \quad (28)$$

This is precisely Eq. (25) with $B=\beta/2$ as discussed in the previous section.

Due to the presence of current velocity in the equation, the dependence of $\overline{(\nabla\zeta)^2}$ on wind speed becomes less obvious. In fact, even without current and with contribution from capillary waves, the dependence of $\overline{(\nabla\zeta)^2}$ on wind will still become saturated at moderate wind speeds as reported by Valenzuela *et al.* (1971) and Miller *et al.* (1972). If, for the time being, we concentrate on gravity waves only, the relationship between $\overline{(\nabla\zeta)^2}$ and wind speed is shown in Fig. 14 with current speed as a parameter. From this figure, it seems that surface roughness is not a good measurement of surface wind. However, Eq. (27) can be plotted in a different way by using wind speed as a parameter; the result is shown in Fig. 15. The sharp slope of the curve immediately reveals the sensitive dependence between $\overline{(\nabla\zeta)^2}$ and current speed especially for moderate currents, probably the prevailing state over most of the ocean. Therefore, we could use the surface roughness parameter as a measure of local current changes.

5. Discussion

A few words of caution are appropriate here. First the present analysis has covered only the gravity wave range. Results obtained so far correspond to a special case studied by Cox and Munk (1954a, b) where capillary waves were entirely absent and the cutoff wavelength was taken to be 30 cm. This state could be simulated by either introducing surface agents or by using low-pass filtering in the processing of the actual field data. The latter seems more feasible.

Second, throughout this analysis, the basic dispersion relation

$$\sigma^2=gk \quad (29)$$

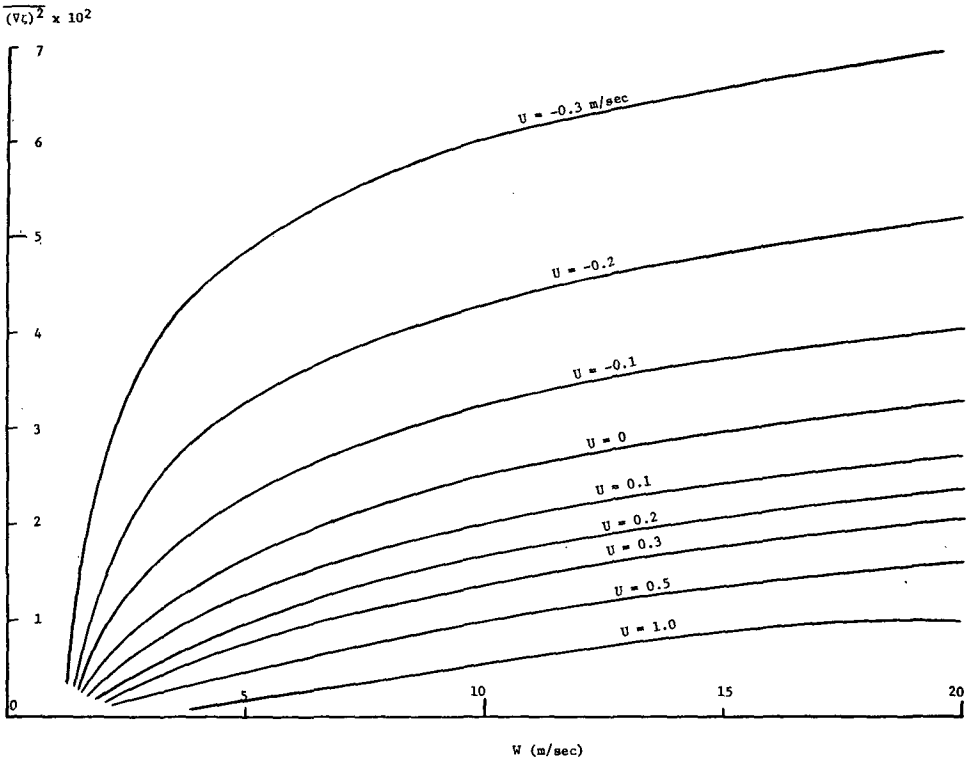

FIG. 14. Variation of rms surface slope with wind speed with current speed as a parameter.

has been used. This implies that the nonlinear wave-wave interaction has been neglected. In fact, this simple dispersion relation is a good approximation even in a random ocean wave field as reported by Longuet-Higgins *et al.* (1963) where there was a 10% increase in wavenumber as compared with that given by Eq. (29).

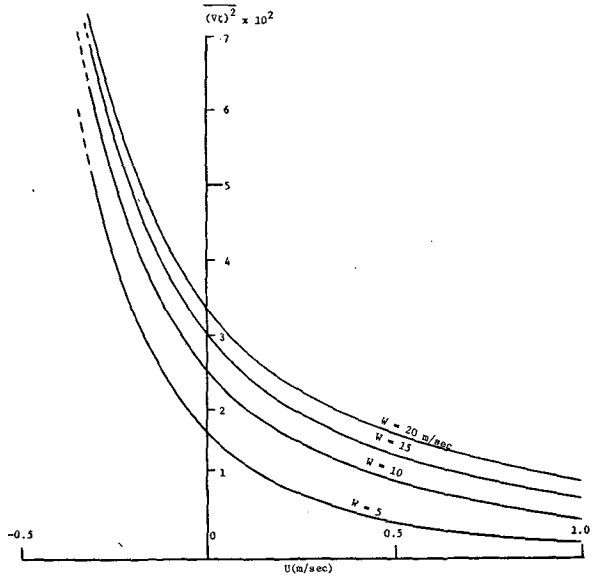

FIG. 15. Variation of rms surface slope with current speed with wind speed as a parameter.

Recent theoretical analyses of Huang and Tung (1972) showed that this 10% deviation could be produced by the nonlinear wave-wave interactions. The maximum deviation due to the wave-wave interaction for an equilibrium range covering two decades of wavenumbers is about 20%, which is substantial but not overwhelming. Another rationale for neglecting the wave-wave interactions is due to the weak nature of the mechanism (see, for example, Phillips, 1966, p. 63ff). Nonlinear wave-wave interaction can indeed redistribute energy in the spectrum, but as far as the overall energy level is concerned, this weak interaction cannot compare in importance with the effective exchange of energy between current and wave motions. If the nonlinear interactions are neglected for the time being, we can regard the wave field as a sum of independent wave components which gives the apparent random surface. On this random surface, though each individual crest and trough is not conserved, the conservative properties will apply to every component or energy band. Improvement can, of course, be made to include such nonlinear mechanisms in the future.

Third, the energy equation is obtained by integrating the Navier-Stokes equation over the depth of water but with dissipation terms neglected (see, for example, Phillips, 1966, p. 47ff). In the ocean wave problem, however, there is additional dissipation due to wave breaking. The breaking phenomenon will cause serious difficulty in the case of a saturated ocean encountering

opposing currents where the vigorous breaking will drain a tremendous amount of energy. Lacking an accurate analytic method to describe such processes, we have to view the curves representing a saturated wave field encountering a strong opposing current with caution. Perhaps actual field data will offer some modification of the theoretical results. More detailed discussion is impossible at present for lack of such data.

Finally, in order that the proposed method for current measurement be practical, a strong gradient of the current field is essential. For example, within the length scale of wave decay there should be appreciable change in current velocity. If we concentrate on the gravity wave case, the time scale of decay, T, is given by

$$T=\frac{1}{\nu k^2}, \tag{30}$$

where ν is the kinematic viscosity of water; therefore, the length scale of decay, L, becomes

$$L=cT=\sqrt{\frac{g}{k}}\frac{1}{\nu k^3}=\frac{\sqrt{g}}{\nu k^{\frac{5}{2}}}. \tag{31}$$

For a minimum wavelength of 30 cm, $k=20$ m^{-1}, this gives $L\approx 1700$ m. Although there are relatively few detailed velocity gradient observations along major ocean systems, cases like those cited by Stommel (1966), where an abrupt velocity change of half a knot exists across sides of sargassum weed, have been observed frequently. Further evidence includes recent results of satellite infrared imagery of the Gulf Stream edge by Rao *et al.* (1971), which also indicate that strong temperature gradients are indeed very common along major ocean systems. Under such conditions, the present method stands a good chance of success.

Granted that the present method can only give relative current values, this, however, can be overcome by utilizing the generalized dispersion relation shown in Fig. 1, provided that the frequency and the wavenumber can be measured independently. All these measurements require only surface parameters accessible by remote sensing techniques. This unique feature offers a possible method for large-scale instantaneous measurement of major ocean current systems.

Acknowledgments. This research is supported in part by the National Oceanic and Atmospheric Administration Sea Grant to the North Carolina State University and in part by the National Aeronautical and Space Administration, Wallops Island Station, under Contract NAS6-2135.

REFERENCES

Cox, C. S., and W. H. Munk, 1954a: Statistics of the sea surface derived from sun glitter. *J. Marine Res.*, **13**, 198–227.

——, and ——, 1954b: Measurements of the roughness of the sea surface from photographs of the sun's glitter. *J. Optical Soc. Amer.*, **44**, 838–850.

Huang, N. E., and C. C. Tung, 1972: The dispersion relation for a nonlinear random gravity wave field. T.R. 72-1, Center for Marine and Coastal Studies, North Carolina State University.

Kitaigorodskii, S. A., 1962: Applications of the theory of similarity to the analysis of wind-generated wave motion as a stochastic process. *Bull. Acad. Sci. USSR, Geophys. Ser.*, **1**, 105–107.

Landau, L. D., and E. M. Lifshitz, 1959: *Fluid Mechanics.* London, Pergamon Press, 536 pp.

Lighthill, M. J., and G. B. Whitham, 1955: On kinematic waves. *Proc. Roy. Soc., London*, **A229**, 281–345.

Longuet-Higgins, M. S., and R. W. Stewart, 1960: Changes in the form of short gravity waves on long waves and tidal currents. *J. Fluid Mech.*, **8**, 565–583.

——, and ——, 1961: The changes in amplitude of short gravity waves on steady non-uniform currents. *J. Fluid Mech.*, **10**, 529–549.

——, and O. M. Phillips, 1962: Phase velocity effects in tertiary wave interactions. *J. Fluid Mech.*, **12**, 333–336.

——, D. E. Cartwright and N. D. Smith, 1963: Observations of the directional spectrum of sea waves using the motions of a floating buoy. *Ocean Wave Spectra*, Englewood Cliffs, N. J., Prentice-Hall, 111–136.

Miller, L. S., G. S. Hayne and G. S. Brown, 1972: Analysis of satellite altimeter signal characteristics and investigation of sea-truth data requirements. Final Report to NASA, Wallops Station, NAS6-1952

Phillips, O. M., 1958: The equilibrium range in the spectrum of wind-generated waves. *J. Fluid Mech.*, **4**, 426–434.

——, 1960: On the dynamics of unsteady gravity waves of finite amplitude, Part I. *J. Fluid Mech.*, **9**, 193–217.

——, 1966: *The Dynamics of the Upper Ocean.* Cambridge University Press, 261 pp.

Pierson, W. J., and L. Moskowitz, 1964: A proposed spectral form for fully developed wind seas based on the similarity theory of S. A. Kitaigorodskii. *J. Geophys. Res.*, **69**, 5181–5190.

Rao, P. K., A. E. Strong and R. Koffler, 1971: Gulf Stream meanders and eddies as seen in satellite infrared imagery. *J. Phys. Oceanogr.*, **1**, 237–239.

Stommel, H., 1966: *The Gulf Stream—A Physical and Dynamical Description.* Berkeley, University of California Press, 248 pp.

Taylor, G. I., 1955: The action of a surface current used as a breakwater. *Proc. Roy. Soc., London*, **A231**, 466–478.

Ursell, F., 1960: Steady wave patterns on a non-uniform steady fluva flow. *J. Fluid Mech.*, **9**, 333–346.

Valenzuela, G. R., M. B. Laing and J. C. Daley, 1971: Ocean spectra for the high-frequency waves as determined from airborne radar measurements. *J. Marine Res.*, **29**, 69–84.

Whitham, G. B., 1960: A note on group velocity. *J. Fluid Mech.*, **9**, 347–352.

——, 1962: Mass, momentum and energy flux in water waves. *J. Fluid Mech.*, **12**, 135–147.